frontiers | Frontiers in Physics

TYPE Original Research
PUBLISHED 22 August 2022
DOI 10.3389/fphy.2022.949571



OPEN ACCESS

EDITED BY
Peng Yan,
University of Electronic Science and Technology of China, China

REVIEWED BY
Lei Bi,
University of Electronic Science and Technology of China, China
Farhad Sattari,
University of Mohaghegh Ardabili, Iran

*CORRESPONDENCE
Hiroyuki Awano,
awano@toyota-ti.ac.jp

SPECIALTY SECTION
This article was submitted to Condensed Matter Physics, a section of the journal Frontiers in Physics

RECEIVED 21 May 2022
ACCEPTED 12 July 2022
PUBLISHED 22 August 2022

CITATION
Matsumoto K, Thach PV, Sumi S, Ranjbar S, Tanabe K, Awano H, Wang S, Ishibashi T and Saito S (2022), Enhancement of permittivity off-diagonal terms in rare earth transition metal / heavy metal hetero-structured films.
*Front. Phys.* 10:949571.
doi: 10.3389/fphy.2022.949571



# Enhancement of permittivity off-diagonal terms in rare earth transition metal / heavy metal hetero-structured films

Kei Matsumoto[1], Pham Van Thach[1,2], Satoshi Sumi[1], Sina Ranjbar[1], Kenji Tanabe[1], Hiroyuki Awano[1]*, Shihao Wang[3], Takayuki Ishibashi[3] and Shin Saito[4]

[1]Department of Advanced Science and Technology, Toyota Technological Institute, Nagoya, Japan, [2]Institute of Materials Science, Vietnam Academy of Science and Technology, Hanoi, Vietnam, [3]Department of Materials Science and Technology, Nagaoka University of Technology, Nagaoka, Japan, [4]Department of Electronic Engineering, Graduate School of Engineering, Tohoku University, Sendai, Japan

The spin Hall effect, Dzyaloshinskii-Moriya interaction, Rashba effect, etc. are extremely important effects for the development of the conduction phenomenon of spin electronics due to the breaking of the spatial inversion symmetry of the hetero interface made of heavy metals such as Pt and W. These are due to SOI (spin-orbit interaction). Most of these studies have been conducted in the frequency domain below GHz, and there are few studies in the energy domain of light. Therefore, in the region of light energy, the magnetic optical Kerr effect spectra of the TbCo/Pt hetero-structured film with large SOI from the Pt interface and the TbCo/Cu hetero-structured film with small SOI from the Cu interface were measured, and the permittivity tensors were investigated respectively. As a result, in the TbCo/Pt hetero-structured film, the dielectric constant off-diagonal component real part of the thin TbCo layer increased about twice as much as that of bulk TbCo in the energy region smaller than 2.5 eV. However, this increase was not observed in the TbCo/Cu hetero-structured film. This result suggests that the influence of the Pt hetero interface where the spatial inversion symmetry is broken may appear even in the energy region of light. Furthermore, it has been confirmed that TbCo/W hetero-structured film using W with a large SOI has the same increasing effect as that of the TbCo/Pt.

KEYWORDS

**hetero-structure, ferrimagnet, spin-orbit interaction, magneto-optics, off-diagonal permittivity**

## Introduction

In recent years, the interesting interfacial effects generated in the heterostructure of the magnetic layer and heavy metal layer have been attracting attention; such as spin injection into the magnetic layer from the heavy metal layer [1, 2], Dzyaloshinskii-Moriya interaction [3, 4], and Rashba effect [5]. The memory, sensor and neuromorphic devices based on these interfacial effects have been invented and studied [6–8]. These interfacial effects originate from the Spin-Orbit Interaction (SOI) which generates in the interface of the heavy metal layer and the magnetic layer. However, the value of some interfacial effects depends on the measurement method [9], and guidelines for increasing the interfacial effect have not yet been clearly obtained. Therefore, further investigation of the interfacial effects is needed.

On the other hand, Magneto-Optical Kerr Effect (MOKE) measurement has been used as a famous method for the non-contact and simple evaluation of magnetic properties in magnetic materials. In recent years, it is also frequently used for spintronics research; to observe domain wall motion in magnetic nanowires, to evaluate spin Hall effect in heavy metals, and to detect spin-orbit torque in magnetic layer/heavy metal layer heterostructures [10–13]. We can also evaluate the off-diagonal part of permittivity, which is the magneto-optical properties that determine the magnitude of the magneto-optical effect, from MOKE measurement [14–19]. In the study of the magneto-optical Kerr spectrum of Co/Pt multilayer films, it is often reported that a very large Kerr rotation angle can be obtained in the ultraviolet region. However, these results have a symmetric structure in the stacking direction, and there are few reports of an asymmetric structure. Also, there is little discussion of the Kerr spectrum in the infrared region. The origin of the magneto-optical Kerr effect in the ultraviolet region is mainly electronic transitions, but the influence of conduction electrons remains in the magneto-optical Kerr effect in the infrared region. Therefore, it is expected that the effect of breaking the spatial inversion symmetry of the hetero interface consisting of heavy metals and magnetic layers may appear in the magneto-optical Kerr effect in the infrared region.

Therefore, Saito's group at Tohoku Univ. Have been reported the magneto-refractive effect of Co/Ru multilayer in the infrared region [20, 21]. They found that a signal similar to the giant magneto-resistance effect due to spin-dependent scattering is detected in the infrared region of the MOKE signal. This is considered to be evidence that the influence of conduction electrons is visible in the infrared region. However, in the visible region, only the normal magnetic hysteresis curve due to optical transition can be observed. If the spin-dependent scattering is caused by interfacial SOI, MOKE is expected to be a highly sensitive and easy method to detect interfacial effects. However, there have been few reports on the changes in magneto-optical properties due to the interfacial effects, because the amount of MOKE signal of the magnetic thin layer is extremely small. To detect the small signal, optical interference effect has been used. Dielectric materials with designed thickness have been prepared above or bottom of the magnetic material so that multiple reflections occur at the top and bottom interfaces of the dielectric layer. These many reflections at the dielectric/magnetic layer interface increase Kerr rotation angle [21]. This method is used to detect recorded data on Magneto-Optical disks with high sensitivity [22], and to facilitate the observation of domain wall motion in ferromagnetic and antimagnetic materials with low net magnetization by MOKE microscopy [23, 24]. Moreover, we have shown that it is possible to enhance the MOKE signal by optical multiple interferences even in magnetic materials as thin as a few nm, and the measured value agrees well with the calculated value using the refractive index method [25]. After that, the difference between measured and calculated MOKE spectra in asymmetric film structures which generate interfacial SOI [26] can be successfully detected. Using this technique, five types of bi-layer films of TbCo/Pt, TbCo/W, TbCo/Ta, TbCo/Ru, and TbCo/Cu are prepared, and the magneto-optical Kerr spectrums are measured. From these results, the off-diagonal dielectric constant tensor $\varepsilon_{xy}$ were investigated. It was found that the real part of the $\varepsilon_{xy}$ of Cu heterostructure sample in the infrared region is the same as the bulk value of the TbCo. This is because the influence of the spin orbital interaction at the hetero interface is small. However, in the case of Pt and W heterostructures, they are larger than that of the bulk TbCo. This is considered to be the effect of the large spin activation interaction from the heavy metal layer of Pt or W due to the hetero interface.

## Experimental methods

The heterostructure samples are prepared using DC or RF magnetron sputtering on a non-doped Si (100) substrates. To enhance the MOKE signal using the optical interference effect in the infrared region, the optimum $SiO_x$ thickness was 100 nm. The signal of the magneto-optical Kerr effect is large in the case of the polar magnetic arrangement. Therefore, in order to easily obtain a perpendicular magnetization film, a rare earth transition metal alloy such as ferrimagnetic TbCo (composition is Tb: Co = 25 : 75) or GdFeCo (composition is Gd: Fe: Co = 20 : 60: 20), was used as the hetero seed layer for the magnetic layer, Pt, W, Ru, Ta with large DMI and SHE were used and Cu with small DMI and SHE was used as the comparison. $SiN_x$ layer was used as a capping layer to prevent oxidation of the magnetic layer. The light wavelength dependence of Kerr rotation angle and ellipticity are measured using a Kerr spectroscopy measurement system [27]. We used the refractive index

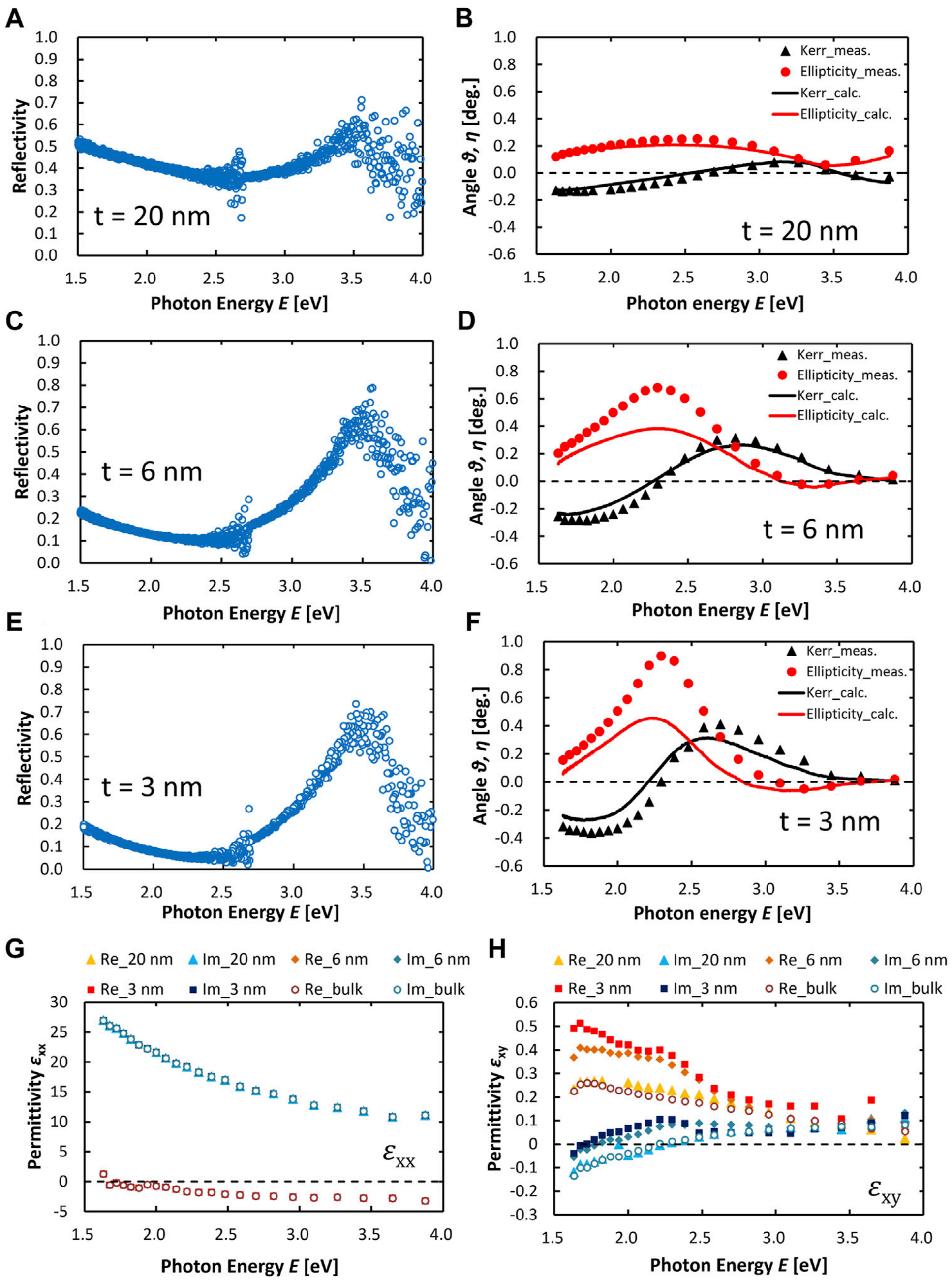


FIGURE 1
**(A–F)** The measured spectra of reflectivity and the calculated and measured spectra of MOKE. The measured spectra (blue hollow circles) of reflectivity of 20 nm-thck TbCo sample **(A)**, 6 nm-thck TbCo sample **(C)** and 3 nm-thck TbCo sample **(E)**. The calculated (solid line) and measured (solid dots) MOKE spectra of 20 nm-thck TbCo sample **(B)**, 6 nm-thck TbCo sample **(D)** and 3 nm-thck TbCo sample **(F)**. Black plots and red plots represent Kerr rotation and ellipticity, respectively. **(G,H)** The permittivity spectra of bulk TbCo (100 nm) and thin film TbCo (20, 6, 3 nm). The diagonal elements **(G)**. The off-diagonal elements **(H)**. The square dots show the permittivity of thin film TbCo and the hollow circle dots show bulk TbCo. Red and yellow plots show the real part of permittivity. Blue plots show the imaginary parts of permittivity.

method to calculate the spectra of MOKE [28]. By using this method, we can calculate the heterostructure's reflectivity of right and left-handed circularly polarized light from the refractive index of bulk material of each layer. The refractive index of the substrate and the layers composing the heterostructure are investigated using an ellipsometry. We measured the refractive index of about 100 nm thick layer films, assuming they would have the same optical properties as the bulk materials. The spectra of MOKE have been calculated using with the light wavelength dependence of the refractive index of each layer in the heterostructure. The all samples show perpendicular magnetized film with square ratio of 1. The structure of the RE-TM layer of all samples was amorphous and the composition was confirmed by EDX.

# Results and discussion

## The photon energy dependence of magneto-optical kerr effect and the off-diagonal terms analysis of the permittivity for the TbCo/Pt hetero-interface films

In order to investigate the effect of the Drude term on the magneto-optical effect at the Pt and TbCo hetero interface, the thickness of the dielectric layer was unified to 100 nm. The reflectance spectra of the sample structure of the $SiN_x$ 10 nm/TbCo t nm/Pt 3 nm/$SiO_x$ 100 nm/Si substrate are shown in Figure 1 (a) t = 20 nm, (c) t = 6 nm, (e) t = 3 nm. In all the results, the reflectance is small at around 2.4 eV, that is, the absorption is large in this region, and the influence of the magneto-optical effect on the TbCo and Pt hetero interface can be emphasized. The spectra of the magneto-optical Kerr rotation angle and the Kerr ellipticity are shown in Figure 1 (b) t = 20 nm, (d) t = 6 nm, (f) t = 3 nm. The magneto-optical Kerr rotation angle is indicated by ▲ points, and the Kerr ellipticity is indicated by ● points. In addition, the spectra obtained by calculating the magneto-optical Kerr rotation angle and Kerr ellipticity using the known optical constants of each layer are also shown by solid lines in the figure. In the result of (b) t = 20 nm, the measured value and the calculated value are in good agreement, and the influence of the hetero interface is not shown. However, when the TbCo thickness becomes as thin as (d) t = 6 nm and (f) t = 3 nm, the Kerr ellipticity around 2.3 eV shows a peak about twice as large as the calculated value. This is considered to be due to the influence of the hetero interface.

However, this increase in Kerr ellipticity may be due to the interference effect of the $SiO_x$ layer. Therefore, in order to remove the influence of the interference effect, the spectra of the diagonal and off-diagonal components of the dielectric constant of the TbCo layer were obtained. The results are shown in Figures 1G,H diagonal term $|\varepsilon_{xx}|$ off-diagonal term $|\varepsilon_{xy}|$. For comparison, the respective spectra of TbCo 100 nm as bulk material are also shown in the figure. The spectra of the real part (Re $|\varepsilon_{xx}|$) and the imaginary part (Im $|\varepsilon_{xx}|$) in the three types of heterostructures with different TbCo film thickness shown in Figure 1G completely overlap with these values of the bulk TbCo. From this result, it can be seen that the interference effect due to the $SiO_x$ layer near 2.4 eV in Figures 1A–F has disappeared. Thus, the $|\varepsilon_{xx}|$ shows the same spectrum at any TbCo thickness, and the effect of the hetero-interfacial Pt layer does not appear. So, what about the effect of the Pt layer on the spectrum of the off-diagonal terms of the permittivity, where the magnetic properties appear? As shown in Figure 1H, the spectrum $|\varepsilon_{xy}|$ at t = 20 nm is almost the same as that of bulk TbCo. However, the $|\varepsilon_{xy}|$ of t = 6 nm and t = 3 nm show larger values than bulk TbCo in the energy region smaller than 2.5 eV. In particular, the increase of the real part Re$|\varepsilon_{xy}|$ is remarkable. It is considered that the influence of the SOI at the hetero interface of the Pt layer is remarkable on the low energy side.

We need to discuss Pt proximity effect in sample structure. As shown the results reported by S. Uba *et al.* [29], it is well known that the magneto-optical Kerr effect of Co/Pt multilayer films increases in the high energy region above 3eV and decreases in the low energy region below 3eV. This paper also shows the proximity effect of Pt in contact with Co, and considers the proximity effect of Pt as one of the causes of the increase in the magneto-optical Kerr effect on the high energy side. Assuming that the Pt proximity effect increases the magneto-optical effect on the high-energy side, the magneto-optical effect on the low-energy side is reduced by the Pt proximity effect. As a result, since the multilayer film structure is Co/Pt/Co/Pt/Co/Pt/Co .., most of the asymmetries of the hetero interface between Co and Pt cancel each other out. Therefore, this result is not an evaluation of the asymmetry of the hetero interface. However, since this magneto-optical effect is the measurement result of one hetero interface of TbCo/Pt, we can discuss the asymmetry effect.

In addition, focusing on the relationship between real and imaginary part of the permittivity, the Kramers–Kronig relation seems be hold. When one crosses the zero axis, the other shows a maximum. For example, the Re$|\varepsilon_{xy}|$ of t = 6 nm film of TbCo has extremely broad peak and Im$|\varepsilon_{xy}|$ crosses the zero axis near 2.0 eV in Figure 1H. The Kramers–Kronig relation seems be hold from this result.

## Dielectric and off-diagonal spectra of dielectric constants in TbCo/Pt, TbCo/W, TbCo/Cu, TbCo/Ta, TbCo/Rh hetero-interfacial bilayer films

If the increase of $|\varepsilon_{xy}|$ in the low energy region of this TbCo (6 nm)/Pt (3 nm) heterostructure film is due to the effect of the Pt layer, similar results should be obtained for W, which has a large SOI as well as Pt. The experimental results of TbCo (6 nm)/W (3 nm) are shown in Figure 2J, and it can be seen that both the real and imaginary parts of $|\varepsilon_{xy}|$ increase in the energy region smaller than 2.5eV, similar to the results of Pt. As in the case of Pt, the increase in the real part Re$|\varepsilon_{xy}|$ is remarkable in the case of W. On the contrary, in the case of TbCo (6 nm)/Cu (3 nm) using Cu with a small SOI [30, 31], this increase of the $|\varepsilon_{xy}|$ should not appear. The experimental results of Cu are shown in Figure 2D, but no increase of the $|\varepsilon_{xy}|$ is observed in any energy region. The small peak in the real part of the $|\varepsilon_{xy}|$ near 2.2 eV in Figure 2D is considered to be due to the influence of the absorption edge of Cu. Thus, the spectral measurement of the $|\varepsilon_{xy}|$ is effective method for investigating the influence of the hetero interface. Therefore, we conducted similar experiments with TbCo

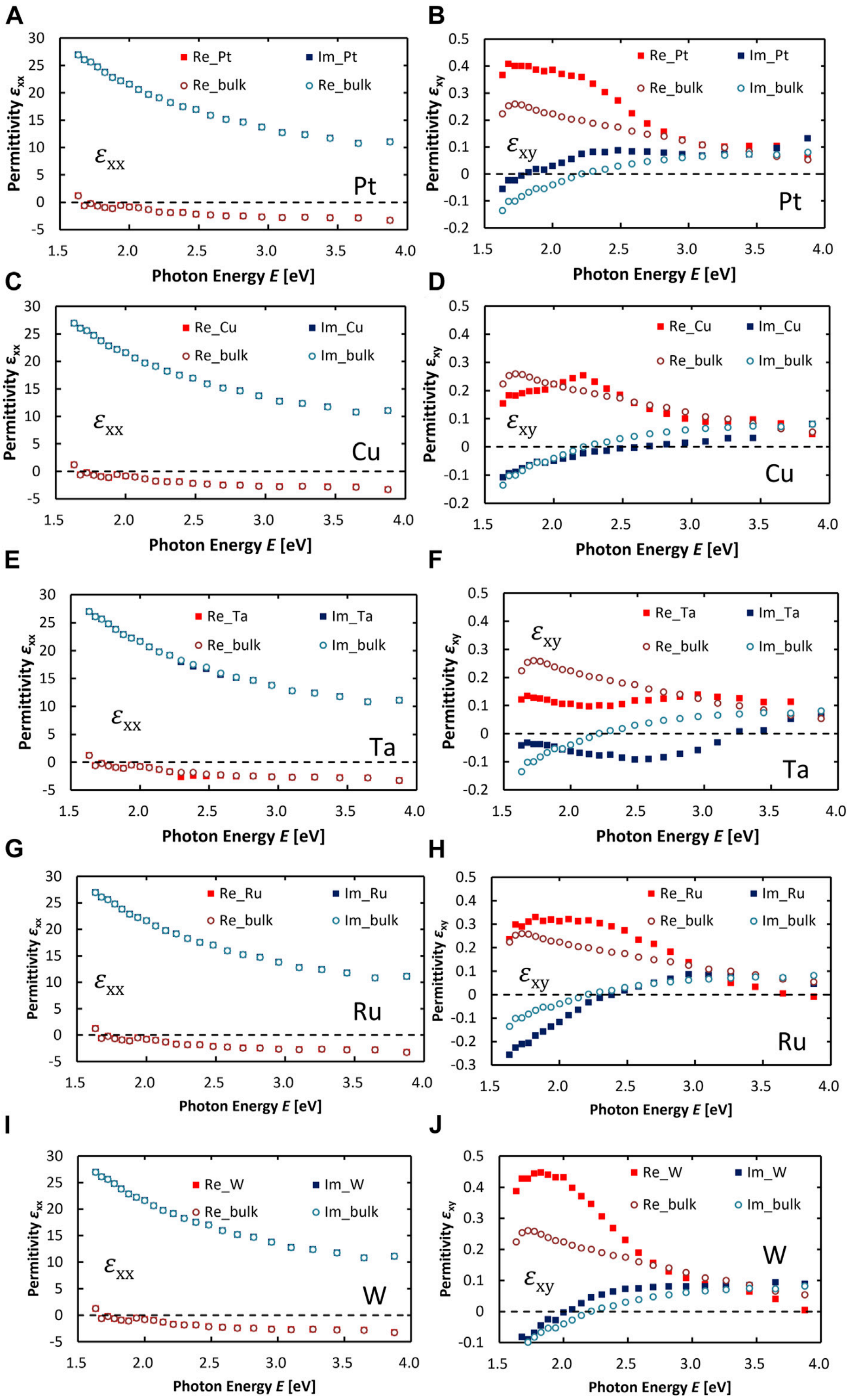


FIGURE 2
The permittivity spectra of bulk TbCo(100 nm) and thin film TbCo(6 nm). The diagonal elements of Pt-under layer sample **(A)**. The off-diagonal elements of Pt-under layer sample **(B)**. The diagonal elements of Cu-under layer sample **(C)**. The off-diagonal elements of Cu-under layer sample **(D)**. The diagonal elements of Ta-under layer sample **(E)**. The off-diagonal elements of Ta-under layer sample **(F)**. The diagonal elements of Ru-under layer sample **(G)**. The off-diagonal elements of Ru-under layer sample **(H)**. The diagonal elements of W-under layer sample **(I)**. The off-diagonal elements of W-under layer sample **(J)**. The square dots show the permittivity of thin film TbCo and the hollow circle dots show bulk TbCo. Red and blue plots show the real part and the imaginary part of permittivity, respectively.

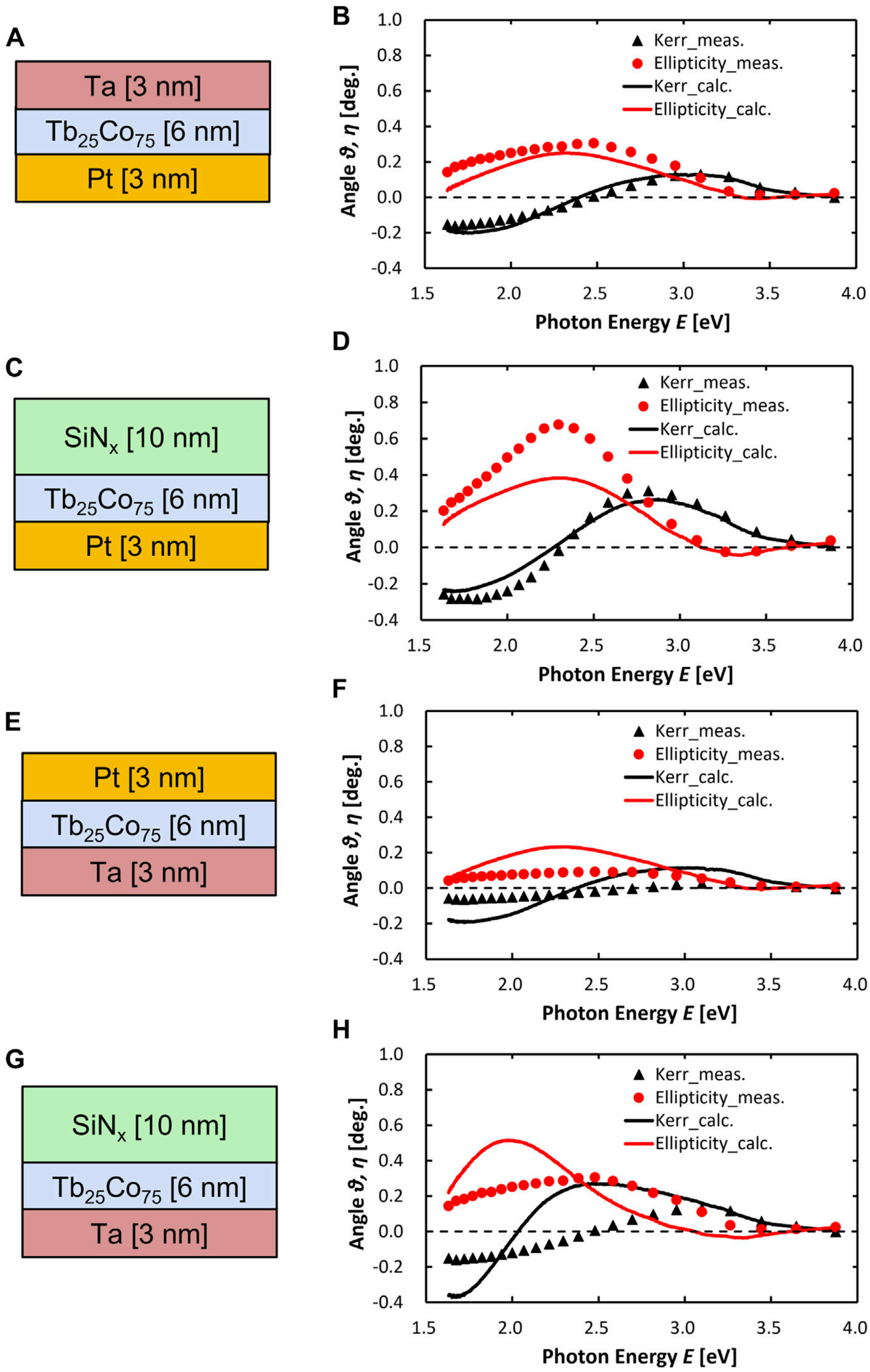


FIGURE 3
The sample structure and the calculated and measured MOKE spectra. **(A–D)** The results of Pt-under layer sample. The structure of Pt-under layer sample with Ta-cap layer **(A)** and $SiN_x$-cap layer **(C)**. The calculated (solid line) and measured (solid dots) MOKE spectra of the Ta-cap layer sample **(C)** and $SiN_x$-cap layer sample **(D)**. **(E–H)** The results of Ta-under layer sample. The structure of Ta-under layer sample with Pt-cap layer **(E)** and $SiN_x$-cap layer **(G)**. The calculated and measured MOKE spectra of the Pt-cap layer sample **(F)** and $SiN_x$-cap layer sample **(H)**. Black plots and red plots represent Kerr rotation and ellipticity, respectively.

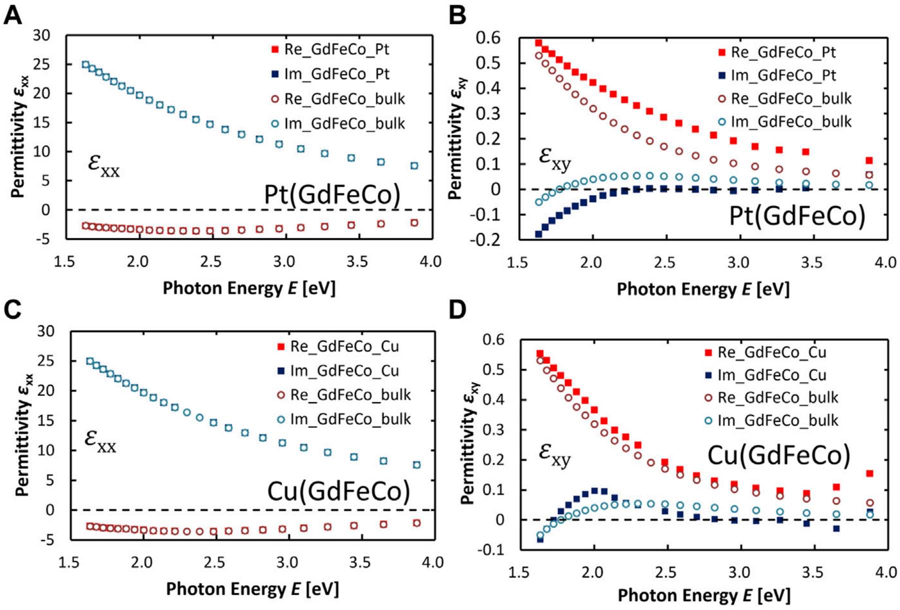


FIGURE 4
The permittivity spectra of bulk GdFeCo (100 nm) and thin film GdFeCo (6 nm). The diagonal elements of Pt-under layer sample **(A)**. The off-diagonal elements of Pt-under layer sample **(B)**. The diagonal elements of Cu-under layer sample **(C)**. The off-diagonal elements of Cu-under layer sample **(D)**. The square dots show the permittivity of thin film and the hollow circle dots show bulk GdFeCo. Red and blue plots show the real part and the imaginary part of permittivity, respectively.

(6 nm)/Ru (3 nm) and TbCo (6 nm)/Ta (3 nm) hetero-structured films. It is known that the influence of the hetero interface of SOI of Ru and Ta is not as great as that of Pt and W. As shown in Figure 2H Ru, the increase of the Re$|\varepsilon_{xy}|$ in the lower energy region can be seen, however the value is not so remarkable. This result can be attributed to Ru's DMI being smaller than that of Pt [32]. On the other hand, in the case of TbCo/Ta in Figure 2F, on the contrary, the Re$|\varepsilon_{xy}|$ decreases in the low energy region compared to bulk TbCo, and the Im$|\varepsilon_{xy}|$ decreases in the medium energy region. It is generally known that the effect of large SOI created by this Pt interface with broken spatial inversion symmetry appears as an electron conduction phenomenon in a very small energy region. However, it would be surprising if it could be observed even in the low energy region of light.

## Stacked structure dependence of the diagonal and off-diagonal spectra of the permittivity in the X/TbCo/Y hetero-structured film (X, Y: Ta, $SiN_x$, Pt)

The above results were all the results of the Pt base layer and the $SiN_x$ cap layer. As shown in Figure 3D , in the case of the Pt base layer, the Kerr ellipticity peaked at around 2.3 eV, which was larger than the calculation result. On the other hand, in the case of the Ta base layer in Figure 3H, the Kerr ellipticity had a peak near 1.9 eV, and the value was smaller than the calculated value. Then, what happens in the case of the Ta cap layer and Pt base layer? The result is shown in Figure 3B. Since the ellipticity increases in the Pt base decreases in the Ta cap layer, the spectrum of the ellipticity becomes almost the same as the calculated value. The reverse structure is shown in Figure 3H, but the experimental value is smaller than the calculated value. In this way, it was found that the spectrum changes significantly even in the positional relationship between the base layer and the cap layer at the hetero interface.

## Dielectric and off-diagonal spectra of the dielectric constant of GdFeCo/Pt and GdFeCo/Cu heterostructured films with small spin-orbit interaction Gd

Is the increase in the $|\varepsilon_{xy}|$ in the low energy region of the TbCo/Pt heterostructure film related to Tb having a large orbital magnetic moment and a large spin-orbit interaction? Therefore, a GdFeCo/Pt hetero-structured film using Gd without orbital magnetic moment was prepared, and the spectra of the $|\varepsilon_{xx}|$ and $|\varepsilon_{xy}|$ were investigated. The respective results are shown in Figures 4A,B. For comparison, the spectra of GdFeCo/Cu using Cu with small SOI are also shown in Figures 4C,D. The $|\varepsilon_{xx}|$ spectra of GdFeCo/Pt and GdFeCo/Cu both showed good

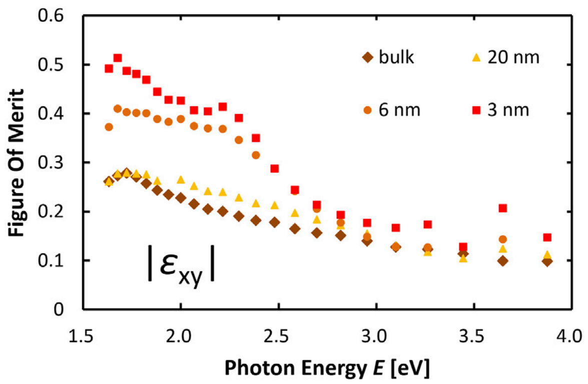


FIGURE 5
The Figure of merit $|\varepsilon_{xy}|$ of the different thickness (bulk (brown dots), 20 nm (yellow dots), 6 nm (orange dots), 3 nm (red dots)) of TbCo layer samples.

agreement with the spectra of bulk GdFeCo. In addition, the Re$|\varepsilon_{xy}|$ of GdFeCo/Pt was slightly above the value of bulk GdFeCo and slightly below the Im$|\varepsilon_{xy}|$ in the entire energy range. This result is different from TbCo/Pt, and the small spin-orbit interaction of Gd may lead to a broad spectrum without peaks. On the other hand, the results of GdFeCo/Cu almost overlapped with the calculated values in the entire energy range, and the results were similar to those of TbCo/Cu.

## Thickness dependence of TbCo figure of merit

It was found that the off-diagonal terms of the permittivity of TbCo/Pt and TbCo/W hetero-structured films are significantly higher than the values of bulk TbCo in the low energy region. In order to apply this result as a magneto-optical device, it is necessary to investigate the Figure of Merit (FOM), which is the product of the dielectric constant off-diagonal term and the reflectance. R. Gamble *et al.* reported that the upper limit of FOM of any structure which includes the magnetic layer is proportional to the absolute value of off-diagonal of permittivity, $|\varepsilon_{xy}|$ [33]. The figure of merit spectrum is shown in Figure 5. As shown in Figures 1A,C,E, the reflectance of all films was low in the low energy region, but the figure of merit of the TbCo/Pt heterostructured film with thinner TbCo layer thickness increased remarkably compared with that of bulk TbCo. When the TbCo film thickness is 3 nm, the figure of merit doubles compared to bulk TbCo, indicating that the heterostructure with Pt is beneficial for application. On the other hand, when the TbCo film thickness is 20 nm, no benefit is seen because the value is equivalent to that of bulk TbCo.

## Conclusion

In summary, we investigated whether the influence of the hetero interface of TbCo/Pt appears in the spectrum of the magneto-optical Kerr effect. The spectra of the permittivity diagonal terms $|\varepsilon_{xx}|$ of the thin TbCo layer of the hetero-structured film were in good agreement with the spectra of the bulk TbCo. On the other hand, the spectrum of the dielectric constant off-diagonal term $|\varepsilon_{xy}|$ of the thin TbCo layer of the hetero-structure film increased twice as much as the spectrum of the bulk TbCo only in the low energy region. This may be due to the large SOI created by the Pt interface with broken spatial inversion symmetry. This increase of the $|\varepsilon_{xy}|$ was also confirmed in the TbCo/W hetero-structured film using W showing a large SOI. On the contrary, in the TbCo/Cu hetero-structured film using Cu showing only a small SOI, this increase of the $|\varepsilon_{xy}|$ was not observed. Thus, the increase of the $|\varepsilon_{xy}|$ on the low energy region is considered to depend on the magnitude of the SOI created by the hetero-structure with broken spatial inversion symmetry. It is generally known that the effect of large SOI created by this Pt interface with broken spatial inversion symmetry appears as an electron conduction phenomenon in a very small energy region. However, it would be surprising if it could be observed even in the low energy region of light.

These were the result of a heterostructured film made of a thin TbCo alloy containing Tb with a large orbital magnetic moment. Therefore, the $|\varepsilon_{xy}|$ spectra of the GdFeCo/Pt heterostructured film and the GdFeCo/Cu heterostructured film using Gd in which the orbital magnetic moment has disappeared were investigated. The $|\varepsilon_{xy}|$ of GdFeCo/Pt was higher than that of bulk GdFeCo, and the $|\varepsilon_{xy}|$ of GdFeCo/Cu was the same as that of bulk GdFeCo. From this result, the characteristics of the Pt heterointerface and the Cu heterointerface with broken spatial inversion symmetry could be reproduced. However, the increase in $|\varepsilon_{xy}|$ due to this Pt hetero interface was slight and appeared in the entire energy range. Moreover, when the figure of merit of the magneto-optical effect of the TbCo/Pt heterostructure film was calculated in the low energy region, it was found that the value was about twice as large as that of the bulk TbCo. Generally, in order to electrically measure SOI such as DMI and SHE of a hetero-magnetic structure with broken spatial inversion symmetry, it is necessary to microfabricate the sample using an expensive equipment. However, if the SOI can be measured with light, they can be easily evaluated without expensive sample processing. For that purpose, it is necessary to construct a theory to identify the SOI from the measurement results of the magneto-optical effect (increase in the off-diagonal term of the permittivity) in the long wavelength region. We hope that this proposal will contribute to the development of spintronics.

## Data availability statement

The datasets presented in this study can be found in online repositories. The names of the repository/repositories and accession number(s) can be found in the article/Supplementary Material.

## Author contributions

HA conceived the idea of the study. KM and PT fabricated the sample. KM and SS measured and analysed the MOKE spectra of the samples. KM and HA drafted the original manuscript. All authors deeply discussed the results of this study and approved the final version of the manuscript for submission.

## Funding

This work was partly supported by a Grant-in-Aids for Scientific Research (17H03240, 20H02185, 21K18735) from JSPS.

## Acknowledgments

The author thanks Ahmet Yagmur for valuable discussion.

## Conflict of interest

The authors declare that the research was conducted in the absence of any commercial or financial relationships that could be construed as a potential conflict of interest.

## Publisher's note

All claims expressed in this article are solely those of the authors and do not necessarily represent those of their affiliated organizations, or those of the publisher, the editors and the reviewers. Any product that may be evaluated in this article, or claim that may be made by its manufacturer, is not guaranteed or endorsed by the publisher.

## References

1. Pai C, Liu L, Li Y, Tseng HW, Ralph DC, Buhrman RA. Spin transfer torque devices utilizing the giant spin Hall effect of tungsten. *Appl Phys Lett* (2012) 101: 122404. doi:10.1063/1.4753947

2. Emori S, Bauer U, Ahn SM, Martinez E, Beach GSD. Current-driven dynamics of chiral ferromagnetic domain walls. *Nat Mater* (2013) 12:611–6. doi:10.1038/nmat3675

3. Ryu K, Thomas L, Yang SH, Parkin S. Chiral spin torque at magnetic domain walls. *Nat Nanotechnol* (2013) 8:527–33. doi:10.1038/nnano.2013.102

4. Ma X, Zhang L, Chang CC, Hung HH, Scalettar RT. Localization of interacting Dirac fermions. *Phys Rev Lett* (2018) 120:116601. doi:10.1103/physrevlett.120.116601

5. Yaji K, Ohtsubo Y, Hatta S, Okuyama H, Miyamoto K, Okuda T, et al. Large Rashba spin splitting of a metallic surface-state band on a semiconductor surface. *Nat Commun* (2010) 1:17. doi:10.1038/ncomms1016

6. Kurokawa Y, Shibata R, Awano H. Novel magnetic wire fabrication process by way of nanoimprint lithography for current induced magnetization switching. *AIP Adv B* (2017) 7:055930. doi:10.1063/1.4977769

7. Woo S, Litzius K, Kruger B, Im MY, Caretta L, Richter K, et al. Observation of room-temperature magnetic skyrmions and their current-driven dynamics in ultrathin metallic ferromagnets. *Nat Mater* (2016) 15:501–6. doi:10.1038/nmat4593

8. Zahedinejad M, Fulara H, Khymyn R, Houshang A, Dvornik M, Fukami S, et al. Memristive control of mutual spin Hall nano-oscillator synchronization for neuromorphic computing. *Nat Mater* (2021) 21:81–7. doi:10.1038/s41563-021-01153-6

9. Kuepferling M, Casiraghi A, Soares G, Durin G. Measuring interfacial Dzyaloshinskii-Moriya interaction in ultra thin films. *arXiv:2009.11830v1* (2020).

10. Klaui M, Jubert PO, Allenspach R, Bischof A, Bland JAC, Faini G, et al. Direct observation of domain-wall configurations transformed by spin currents. *Phys Rev Lett* (2005) 95:026601. doi:10.1103/PhysRevLett.95.026601

11. van't Erve OMJ, Hanbicki AT, McCreary KM, Li CH, Jonker BT. Optical detection of spin Hall effect in metals. *Appl Phys Lett* (2014) 104:172402. doi:10.1063/1.4874328

12. Marui Y, Kawaguchi M, Hayashi M. Optical detection of spin–orbit torque and current-induced heating. *Appl Phys Express* (2018) 11:093001. doi:10.7567/apex.11.093001

13. Montazeri M, Upadhyaya P, Onbasli MC, Yu G, Wong KL, Lang M, et al. Magneto-optical investigation of spin–orbit torques in metallic and insulating magnetic heterostructures. *Nat Commun* (2015) 6:8958. doi:10.1038/ncomms9958

14. Allen R, Connell GAN. Magneto-optic properties of amorphous terbium-iron. *J Appl Phys* (1982) 53:2353–5. doi:10.1063/1.330970

15. Sato K. Proceedings of magneto-optical recording international symposium '92. *J Magn Soc Jpn* (1993) 17:11.

16. Tosaka Y, Ikekame H, Urago K, Kurosawa S, Sato K, Shin S. Magneto-optical spectra in Pd/Co multilayers and related alloys. *J Magn Soc Jpn* (1994) 18:389–92. doi:10.3379/jmsjmag.18.389

17. Lee SL, Lange RJ, Canfield PC, Harmon BN, Lynch DW. Optical and magneto-optical properties of $RFe_2$ ($R$ = Gd, Tb, Ho, Lu) and $GdCo_2$. *Phys Rev B* (2000) 61:9669. doi:10.1103/PhysRevB.61.9669

18. Jesenska E, Hashinaka T, Ishibashi T, Beran L, Dušek J, Antoš R, et al. Optical and magneto-optical properties of Gd22Fe78 thin films in the photon energy range from 1.5 to 5.5 eV. *Materials* (2016) 9:23.

19. Jesenska E, Ishibashi T, Beran L, Pavelka M, Hamrle J, Antoš R, et al. Optical and magneto-optical properties of $Gd_xFe_{(100-x)}$ thin films close to the compensation point. *Sci Rep* (2019) 9:16547. doi:10.1038/s41598-019-52252-z

20. Sato H. *IEEE Trans Found Mat* (2016) 134(4):174.

21. Saito S, Sato H, Ooki K, Akahane K, Uchida H. Near-infrared magneto-refractive effect for antiferro-magnetically exchange coupled Co/Ru multilayer film in transmission configuration. *J Magn Soc Jpn* (2019) 43:25–8. doi:10.3379/msjmag.1903r003

21. Chen T. Wavelength response of harmonic distortion in AC-bias recording. *IEEE Trans* (1980) 16:501. doi:10.1109/TMAG.1980.1060649

22. Mansuripur M. Figure of merit for magneto-optical media based on the dielectric tensor. *Appl Phys Lett* (1986) 49:19–21. doi:10.1063/1.97087

23. Bang D, Yu J, Qiu X, Wang Y, Awano H, Manchon A, et al. Domain wall dynamics in easy-cone magnets. *Phys Rev B* (2016) 93:174424.

24. Tanaka M, Shimazaki M, Ohmasa T, Suzuki T, Honda S, Honda S, et al. Stabilization of Néel-type domain walls in multilayered magnetic wires using antiferromagnetic interlayer exchange coupling. *J Appl Phys* (2020) 128:063902. doi:10.1063/5.0013481

25. Sumi S, Awano H, Hayashi M. Interference induced enhancement of magneto-optical Kerr effect in ultrathin magnetic films. *Sci Rep* (2018) 8:776. doi:10.1038/s41598-017-18794-w

26. Iemoto S, Sumi S, Van Thach P, Awano H, Hayashi M. Interference induced enhancement of magneto-optical effect in Pt/TbCo hetero-structured films. *Crystals* (2018) 8:377. doi:10.3390/cryst8100377

27. Sato K. Measurement of magneto-optical Kerr effect using piezo-birefringent modulator. *Jpn J Appl Phys* (1981) 20:2403–9. doi:10.1143/jjap.20.2403

28. Egashira K, Yamada T. Kerr-effect enhancement and improvement of readout characteristics in MnBi film memory. *J Appl Phys* (1974) 45:3643–8. doi:10.1063/1.1663831

29. Uba S, Uba L, Yaresko AN, Perlov AY, Antonov VN, Gontarz R. Optical and magneto-optical properties of Co/Pt multilayers. *Phys Rev B* (1996) 53:6526–35. doi:10.1103/physrevb.53.6526

30. Ando K, TakahaShi S, Harii K, Sasage K, Ieda J, Maekawa S, et al. Electric manipulation of spin relaxation using the spin Hall effect. *Phys Rev Lett* (2008) 101:036601. doi:10.1103/PhysRevLett.101.036601

31. An H, Kageyama Y, Kanno Y, Enishi N, Ando K. Spin–torque generator engineered by natural oxidation of Cu. *Nat Commun* (2016) 7:13069. doi:10.1038/ncomms13069

32. Ščepka T, Neilinger P, Samardak AS, Kolesnikov AG, Ognev AV, Sadovnikov AV, et al. Damping in Ru/Co-based multilayer films with large Dzyaloshinskii-Moriya interaction. *arXiv:1911.02467v1* (2019).

33. Gamble R, Lissberger P, Parker M. A simple analysis for the optimization of the normal polar magneto-optical Kerr effect in multilayer coatings containing a magnetic film. *IEEE Trans Magn* (1985) 21:1651–3. doi:10.1109/tmag.1985.1063908